



Uncertainty Analysis of Bistable Vibration Energy Harvesters Based on the Improved Interval Extension

Yi Li¹ · Shengxi Zhou¹ · Grzegorz Litak²

Received: 3 November 2018 / Revised: 10 May 2019 / Accepted: 15 May 2019 / Published online: 30 May 2019
© The Author(s) 2019

Abstract

Purpose High-energy interwell oscillations of the bistable energy harvester (BEH) lead to large-amplitude output voltage. For processing and manufacturing of the BEH, small errors and deviations in the final structure cannot be totally eliminated in practice, which will make the output voltage to be apart away from the design value. Therefore, the geometrical variables, material properties and other parameters should be treated as uncertainties in analysis and are bound to their design.

Method This paper presents uncertainty analysis of the BEH to reveal the influence of the uncertain system parameters on the energy harvesting performance. The improved interval extension based on the first-order Taylor series is used to predict the lower and upper bounds of the stable high-energy interwell output voltage of the BEH. In detail, uncertain mass, nonlinear stiffness term, damping, capacitance and electromechanical coupling coefficient are considered. Meanwhile, the Monte Carlo simulation is employed to verify the suitability and the accuracy of this method. Especially, this method allows researchers to define the number of the parameter α_j according to the categories of uncertain variables.

Results The research works show that interval of the output voltage of the BEH can be limited by reducing the number of uncertain variables, and the uncertainty of the output voltage is more sensitive to the electrical uncertain variables than the structural uncertainties.

Conclusion Designers of the BEH should pay enough attention to the errors and tolerances of the electrical output design variables. Specifically, in the design of the BEH, it is more effective to improve the accuracy of the output voltage by limiting the uncertainties of electric parameters than structural parameters. Reducing the number of uncertain parameters through increasing processing precision in production of the BEH can also improve the accuracy of the output voltage.

Keywords Vibration energy harvesting · Uncertainty · Bistable energy harvester · Improved interval extension · System parameters

Introduction

As the rapid development of new materials and electronics in the last 10 years, more and more low-powered embedded electromechanical devices and wireless sensors are used for structural health monitoring [1–4]. In order to power them continuously and realize autonomic health monitoring,

energy harvesting techniques and fault diagnosis methods have been developed recently [5–8]. For example, different flow energy harvesters were designed to power the sensors embedded in high buildings or underwater environments [9–15]. For the high-performance energy harvesting from base vibrations, nonlinear mechanisms have been widely used to design suitable energy harvesters, such as internal resonance mechanism [16, 17], bistable mechanism [18, 19], tristable mechanism [20, 21], and multi-stable mechanism [22, 23].

Fairly high-energy oscillations of the mechanical resonator and large-amplitude output voltage from a Duffing-like bistable energy harvester were experimentally found by Erturk and Inman [24]. This demonstrates the high-efficiency advantage of the bistable energy harvester (BEH) over the traditional linear one. Zhou et al. [25] designed

✉ Shengxi Zhou
zhoushengxi@nwpu.edu.cn

✉ Grzegorz Litak
g.litak@pollub.pl

¹ School of Aeronautics, Northwestern Polytechnical University, Xi'an 710072, China

² Department of Automation, Lublin University of Technology, Nadbystrzycka 36, 20-618 Lublin, Poland

a rotatable nonlinear magnetic coupled energy harvester, which exhibits bistable characteristics for a suitable angle of inclination. Under different harmonic base excitations, the hysteresis and the multi-solution range of the BEH were numerically and experimentally observed. Based on this design, Cao et al. [26] developed a BEH with the nonlinear time-varying potential to efficiently harvest energy from human motions. Litak et al. [27] numerically and experimentally verified the high-efficiency energy harvesting performance of BEHs from random base excitations. Stanton et al. [28] derived a distributed parameter model of magnetic coupled cantilever-based BEH to predict the output voltage and nonlinear response characteristics. Meanwhile, plate-based BEH was presented by Arrieta et al. [29], and this BEH performs well under very high-level base excitations.

For processing and manufacturing of BEHs, the errors cannot be totally eliminated in practice. Therefore, the geometrical variables, material properties and other parameters should be treated as uncertainties in analysis and are bound to their design. For the piezoelectric energy harvester, the mass, the stiffness, the damping, the capacitance, the electromechanical coupling coefficient, etc., are all uncertain variables in design, and these uncertainties can make the output voltage fluctuate around its expected value. In order to analyze this problem, Ali et al. [30] used the Monte Carlo simulation (MCS) to study the effect of parametric uncertainty in the piezoelectric energy harvester on the harvested power and found that the maximum of the mean harvested power decreases with increasing uncertainty. Franco and Varoto [31] used the MCS to research the effects of uncertainties on the performance of the cantilever-based piezoelectric energy harvesters, and they strongly suggested that uncertainties must be accounted for in the design. Brian et al. [32] presented systematic uncertainty propagation studies for both linear and nonlinear energy harvesters. In these studies, uncertainties from the system and environmental excitation were all simulated.

However, in above researches, the probabilistic uncertain analysis method, the MCS, was adopted to obtain accurate distributions of responses. In this case, numerous samples of uncertain variables are needed to define the probability density functions of the uncertain parameters. Therefore, it is very difficult to obtain the enough samples in practice. To partly ameliorate this problem, the interval analysis may be more suitable, because it just needs to know the upper and lower bounds of uncertain variables. Many interval analysis methods have been developed, among which the Taylor expansion [33, 34] is a popular one. It can give the bounds of function based on the sensitivities with respect to the uncertain variables and the deviations, and it does not need to modify the governing function of system. When the dependence of the response on uncertain parameters is non-monotonic in interval, the interval of response will

exhibit significant errors; to limit the errors, Li and Xu [35] defined several cases according to the relationship between the response and uncertain parameter and improved the formats of interval extension based on the first Taylor series correspondingly. To solve practical complex problem, Li et al. recently used parameter $\sin \alpha$ to improve the interval extension based on the first-order Taylor series and provided an opportunity to account for the different categories of uncertainties by defining multiple α_i ($i = 1, 2, \dots$), and consequently the accurate interval of response was obtained by maximizing and minimizing a continuous function [36, 37], respectively. Therefore, this improved interval extension method is used in this paper to investigate the effect of uncertain parameters on the output voltage in the BEH.

In this paper, we use the improved interval extension to make uncertainty analysis of the BEH with uncertain parameters. In “[Theoretical Solutions of the Output Voltage of the BEH](#),” the theoretical solutions of the BEH are provided. In “[Improved Interval Extension Based on the First-Order Taylor Series](#),” the improved interval extension based on the first-order Taylor series is introduced in detail. In “[Effect of the Structural and Electric Parameters on the Output Voltage](#),” the effect of the structural and electric parameters on the output voltage is analyzed. In “[Uncertainty Analysis of the BEH with Uncertain Parameters](#),” the detailed uncertainty analysis of the BEH with uncertain parameters is provided. Conclusions follow in “[Conclusions](#).”

Theoretical Solutions of the Output Voltage of the BEH

The schematic diagram of a general magnetic coupled BEH is shown in Fig. 1. The middle position of the BEH is unstable, while the two bilateral positions are stable. Under the base displacement excitation $x_b(t)$, the electromechanical model of the BEH can be described by the following equations [38, 39]:

$$m\ddot{x}(t) + c\dot{x}(t) - k_1x(t) + k_3x^3(t) - \theta V(t) = -Nm\ddot{x}_b(t), \quad (1)$$

$$C_p\dot{V}(t) + V(t)R^{-1} + \theta\dot{x}(t) = 0, \quad (2)$$

where $x(t)$, m and c are the tip displacement, the equivalent mass and the equivalent damping of the BEH, respectively. C_p , R , θ and $V(t)$ are the equivalent capacitance, the load resistance, the electromechanical coupling coefficient, the output voltage across R , respectively. $-k_1$ and k_3 are the coefficients of the equivalent linear and nonlinear terms, respectively. N is called the amplitude-wise correction factor for the lumped parameter model [38].

If the BEH is subjected to the base acceleration excitation $A \cos(\omega t)$, the electromechanical model can be rewritten for analysis, as follows:

$$\ddot{x}(t) + \bar{c}\dot{x}(t) - \bar{k}_1x(t) + \bar{k}_3x^3(t) - \bar{\theta}V(t) = NA \cos(\omega t), \quad (3)$$

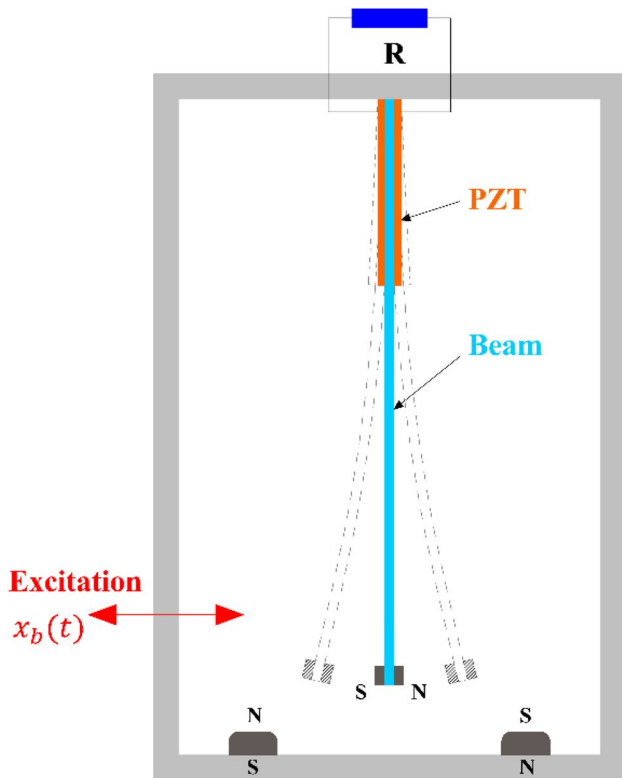


Fig. 1 Schematic diagram of the magnetic coupled BEH in the horizontally moving frame. The piezoelectric bimorph component (PZT) converts the mechanical energy into electrical one

$$C_p \dot{V}(t) + V(t)(R)^{-1} + \theta \dot{x}(t) = 0, \tag{4}$$

where the new parameters are defined as: $\bar{c} = c/m$, $\bar{k}_1 = k_1/m$, $\bar{k}_3 = k_3/m$, $\bar{\theta} = \theta/m$. NA is an effective amplitude of the inertial force.

It is known that the high-energy interwell oscillation of the resonator leads to the large-amplitude output voltage. Therefore, this paper focuses on the steady-state interwell displacement solutions and voltage solutions of the BEH under harmonic-based excitations. For the interwell oscillation, the BEH under base harmonic excitation, the steady-state response displacement and voltage of are assumed to have slowly varying coefficients, described as [39]:

$$x(t) = a(t) \sin(\omega t) + b(t) \cos(\omega t), \tag{5}$$

$$\dot{x}(t) = (\dot{a}(t) - b(t)\omega) \sin(\omega t) + (\dot{b}(t) - a(t)\omega) \cos(\omega t), \tag{6}$$

$$V(t) = C(t) \sin(\omega t) + d(t) \cos(\omega t), \tag{7}$$

$$\ddot{x}(t) = -(2\dot{b}(t) + a(t)\omega)\omega \sin(\omega t) + (2\dot{a}(t) - b(t)\omega)\omega \cos(\omega t), \tag{8}$$

$$\dot{V}(t) = (\dot{C}(t) - d(t)\omega) \sin(\omega t) + (\dot{d}(t) - C(t)\omega) \cos(\omega t), \tag{9}$$

Substituting Eqs. (6), (7) and (9) into Eq. (4), balancing the terms multiplied by $\sin(\omega t)$ and $\cos(\omega t)$, and neglecting all the time derivatives terms, the following equations are obtained:

$$C = \frac{\theta\omega}{\frac{1}{R^2} + (C_p\omega)^2} \left(-C_p\omega a + \frac{b}{R} \right), \tag{10}$$

$$d = \frac{\theta\omega}{\frac{1}{R^2} + (C_p\omega)^2} \left(-\frac{a}{R} - C_p\omega b \right), \tag{11}$$

Substituting Eqs. (5)–(8), (10), (11) into Eq. (3), balancing the terms multiplied by $\sin(\omega t)$ and $\cos(\omega t)$ and neglecting all the time derivatives terms, the following equations are obtained:

$$\left(\frac{3}{4}\bar{k}_3 r^2 - \omega^2 - \bar{k}_1 + SC_p\omega \right) a - \left(\omega\bar{c} + \frac{S}{R} \right) b = 0, \tag{12}$$

$$\left(\frac{3}{4}\bar{k}_3 r^2 - \omega^2 - \bar{k}_1 + SC_p\omega \right) b + \left(\omega\bar{c} + \frac{S}{R} \right) a = NA, \tag{13}$$

where $S = \frac{\bar{\theta}\theta\omega}{\frac{1}{R^2} + (C_p\omega)^2}$.

The final expression of the response displacement and the output voltage are shown as follows:

$$\left(\frac{3}{4}\bar{k}_3 r^2 - \omega^2 - \bar{k}_1 + SC_p\omega \right)^2 r^2 + \left(\omega\bar{c} + \frac{S}{R} \right)^2 r^2 = (NA)^2 \tag{14}$$

$$V = \left| \frac{\theta\omega}{\sqrt{\frac{1}{R^2} + (C_p\omega)^2}} \right| r \tag{15}$$

where r is the response displacement amplitude. V is the response voltage amplitude, $S = \frac{\bar{\theta}\theta\omega}{\frac{1}{R^2} + (C_p\omega)^2}$.

Improved Interval Extension Based on the First-Order Taylor Series

Based on Eqs. (14) and (15), the uncertainty analysis will be performed. This paper will use the improved interval extension based on the first-order Taylor series [36].

In Ref. [36], each uncertain parameter can be described by the interval variable:

$$x^I = [\underline{x}, \bar{x}], \tag{16}$$

where \underline{x} and \bar{x} are the lower and upper bounds of interval, respectively. In addition, x^I can be represented by its central value and deviation, as follows:

$$x_c = \frac{\underline{x} + \bar{x}}{2}, \tag{17}$$

$$\Delta x = \frac{\bar{x} - \underline{x}}{2}. \tag{18}$$

Equation (16) can be rewritten based on the parameterized interval analysis (PIA) [40, 41], as follows:

$$x^I = x_c + \Delta x \sin \alpha, \tag{19}$$

$$\alpha \in \left[-\frac{\pi}{2}, \frac{\pi}{2} \right]. \tag{20}$$

The first-order Taylor expansion of $f(X^I)$ around the central value X_c can be expressed as:

$$f(X^I) \approx f(X_c) + \sum_{i=1}^n \frac{\partial f(X_c)}{\partial x_i} (x_i^I - x_{ic}), \tag{21}$$

where $f(X_c)$ and $\frac{\partial f(X_c)}{\partial x_i}$ are the response at the central values of intervals and the first-order sensitivity of response (at the central values) with respect to the interval variable, respectively.

We substitute Eqs. (19) and (20) into Eq. (21) to build a continuous function with the first-order independent variables, as follows:

$$f(X^I) \approx f(\alpha_j) = f(X_c) + \sum_{i=1}^n \frac{\partial f(X_c)}{\partial x_i} [\Delta x_i \sin \alpha_j]. \tag{22}$$

Equation (22) can be rewritten:

$$f(X^I) \approx f(\alpha_j) = f(X_c) + G(\alpha_j), \tag{23}$$

$$G(\alpha_j) = \sum_{i=1}^n \frac{\partial f(X_c)}{\partial x_i} [\Delta x_i \sin \alpha_j], \tag{24}$$

where j is defined according to the number of categories of uncertainties. The same type of uncertain variables should be expressed by a single α . The bounds of function $f(X^I)$ can be obtained based on the following two equations:

$$\underline{f(X^I)} = f(X_c) + \text{minimum}(G(\alpha_j)), \tag{25}$$

$$\overline{f(X^I)} = f(X_c) + \text{maximum}(G(\alpha_j)). \tag{26}$$

Meanwhile, the first-order sensitivities can be calculated by the common finite-difference method.

$$f'(x) = \frac{f(x+h) - f(x-h)}{2h}, \tag{27}$$

where h is called the finite-difference interval.

Effect of the Structural and Electric Parameters on the Output Voltage

Pervious to uncertain analysis, the effect of the structural and electric variables of the BEH on the output voltage is studied by changing values of these parameters. The base values of the parameters are referred to Ref. [25, 38]. More specifically, the variables are the mass, the nonlinear stiffness, the damping, the capacitance, and the electromechanical coupling coefficient of the BEH. Next, five groups of simulations will be performed. In each case, a specific parameter will be changed by $\pm 2\%$, and the corresponding stable output voltages will calculate based on Eqs. (14) and (15). For system parameters, we used $k_1 = -15.17$ N/m and other specified as central value parameters in Table 1. In additions, only the stable output voltages are plotted in this paper. When the excitation frequency is changing from 8 to 10 Hz to be close to the resonance of interwell solution (the excitation level is 4 m/s^2), the results are shown in Figs. 2, 3, 4, 5 and 6.

It can be found from these figures, the electrical parameters (C_p, θ) have stronger influences on the stable output voltages than the structural parameters (m, k_3, c). Among all these parameters, the influence of the damping c is weakest. Results show that the stable output voltage is increased when we add extra a mass. However, the increase in other parameters makes the output voltage to decrease. In practice, these parameters may be slightly changed at the same time because of manufacturing errors, which will make the output voltage be apart away from the design value. This will bring a negative influence on the energy harvesting performance of the BEH. We should analyze this problem carefully. In the

Table 1 The uncertain parameters

Parameters	Unit	Design value (central value)	Bounds
Mass m^I	kg	6.1219×10^{-3}	$[5.9995 \times 10^{-3}, 6.2444 \times 10^{-3}]$
Nonlinear stiffness term k_3^I	N/m ³	2.6077×10^5	$[2.5555 \times 10^5, 2.6599 \times 10^5]$
Damping c^I	Ns/m	2.4765×10^{-2}	$[2.4270 \times 10^{-2}, 2.5260 \times 10^{-2}]$
Capacitance C_p^I	F	2.9484×10^{-8}	$[2.8894 \times 10^{-8}, 3.0073 \times 10^{-8}]$
Electromechanical coupling coefficient θ^I	N/V	-9.2239×10^{-5}	$[-9.4083 \times 10^{-5}, -9.0394 \times 10^{-5}]$

Fig. 2 The output voltage versus frequency for various mass m

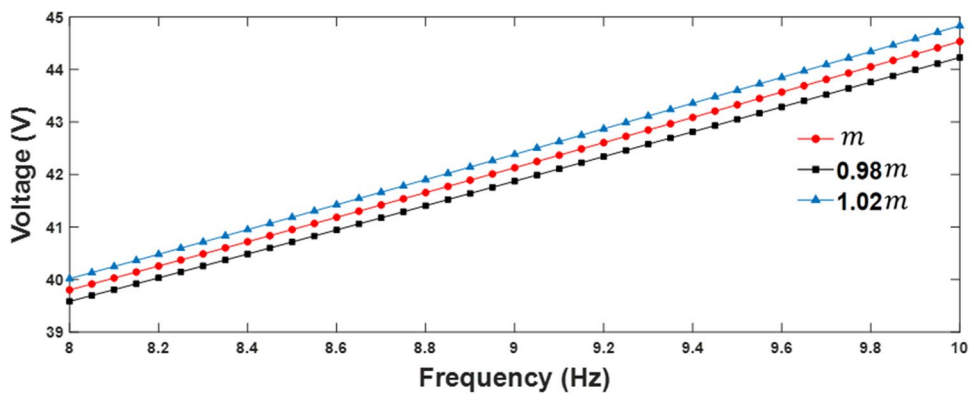


Fig. 3 The output voltage versus frequency for various nonlinear stiffness term k_3

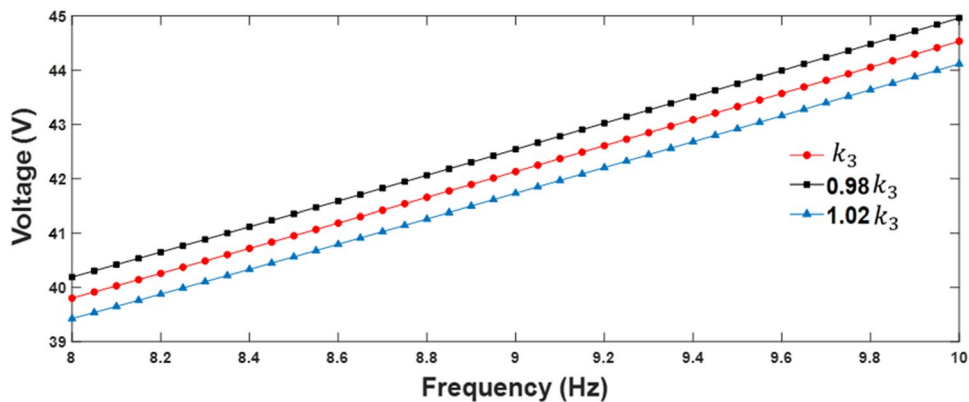


Fig. 4 The output voltage versus frequency for various damping c

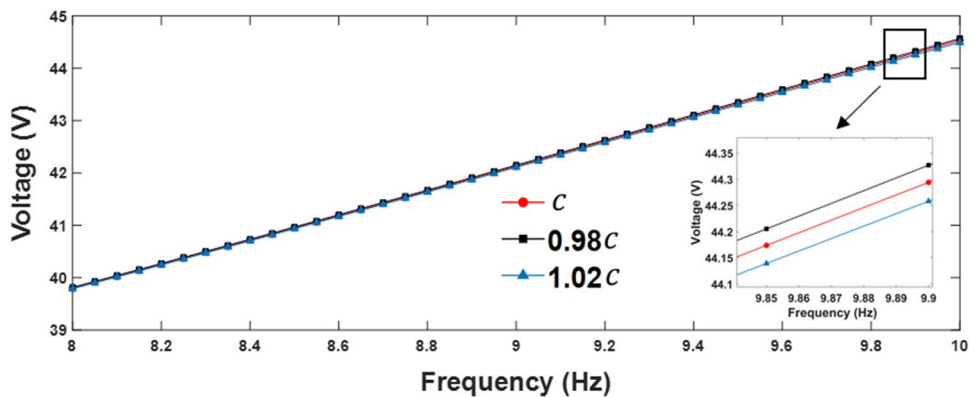


Fig. 5 The output voltage versus frequency for various capacitance C_p

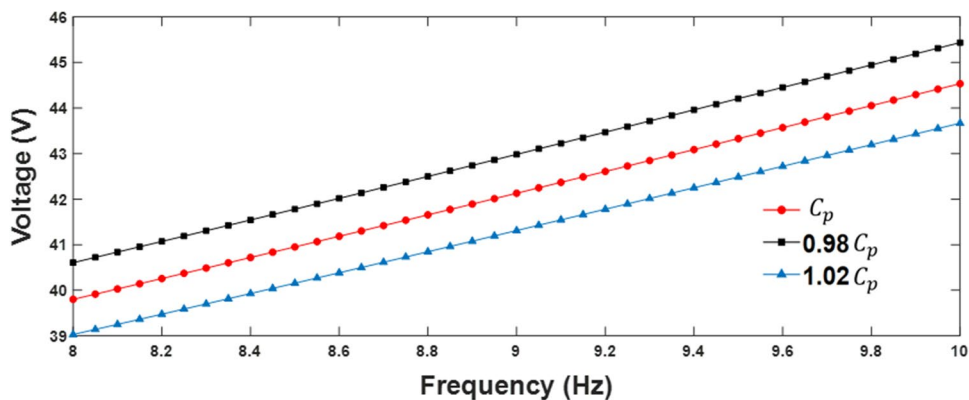
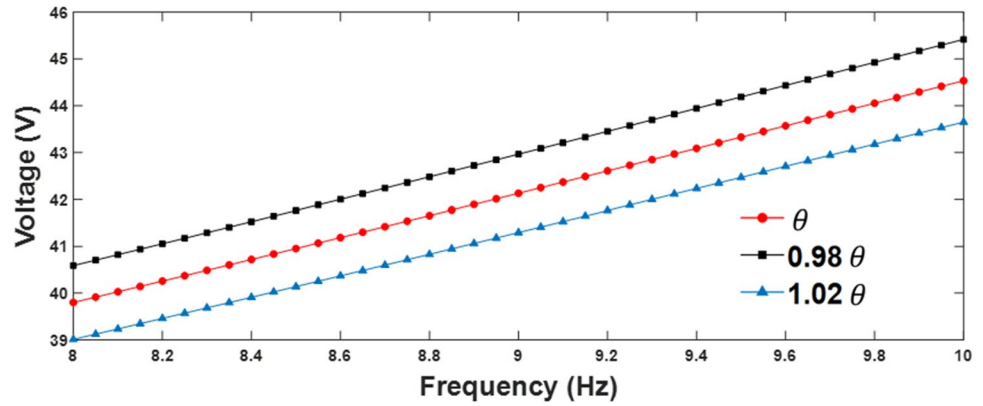


Fig. 6 The output voltage versus frequency for various electromechanical coupling coefficient θ



following section, we use the improved interval extension method to study this effect.

Uncertainty Analysis of the BEH with Uncertain Parameters

According to the results in “Effect of the Structural and Electric Parameters on the Output Voltage,” it is found out that the structural parameters and the electric parameters have remarkable effects on the high-energy interwell output voltage of the BEH. In practical engineering, these parameters may be uncertain due to manufacturing errors. It makes the output voltage deviate from the designed value and become the uncertain variable. Upper and lower bounds of the output voltage can be predicted by the improved interval extension (IIE) based on the first-order Taylor series. The structural uncertainties and the electric uncertainties are described by interval numbers x^l , and they are expressed by m^l, k_3^l, c^l, C_p^l and θ^l to facilitate the understanding, as listed in Table 1. The function $f(X^l)$ is used to calculate the stable output voltage amplitude V .

According to the method illustrated in “Improved Interval Extension Based on the 1st Order Taylor Series,” these interval variables can be expressed by the interval number. m^l and c^l are structural design variables and expressed by the parameter α_1 . k_3^l is strongly influenced by magnets; thus, we use another parameter α_2 to describe it. The rest electrical design variables C_p^l and θ^l are expressed by the parameter α_3 :

$$m^l = [m, \bar{m}] = m_c + \Delta m \cdot \sin \alpha_1, \tag{28}$$

$$c^l = [c, \bar{c}] = c_c + \Delta c \cdot \sin \alpha_1, \tag{29}$$

$$k_3^l = [\underline{k_3}, \bar{k_3}] = (k_3)_c + \Delta k_3 \cdot \sin \alpha_2, \tag{30}$$

$$C_p^l = [\underline{C_p}, \bar{C_p}] = (C_p)_c + \Delta C_p \cdot \sin \alpha_3, \tag{31}$$

$$\theta^l = [\theta, \bar{\theta}] = \theta_c + \Delta \theta \cdot \sin \alpha_3, \tag{32}$$

where $\alpha_1 \in [-\frac{\pi}{2}, \frac{\pi}{2}]$, $\alpha_2 \in [-\frac{\pi}{2}, \frac{\pi}{2}]$, $\alpha_3 \in [-\frac{\pi}{2}, \frac{\pi}{2}]$.

The bounds of the output voltage can be calculated based on Eqs. (25) and (26), as follows:

$$f(m^l, k_3^l, c^l, C_p^l, \theta^l) \approx f(\alpha_1, \alpha_2, \alpha_3) = f(m_c, (k_3)_c, c_c, (C_p)_c, \theta_c) + G(\alpha_1, \alpha_2, \alpha_3), \tag{33}$$

$$G(\alpha_1, \alpha_2, \alpha_3) = \frac{\partial f(m_c, (k_3)_c, c_c, (C_p)_c, \theta_c)}{\partial m} \Delta m \cdot \sin \alpha_1 + \frac{\partial f(m_c, (k_3)_c, c_c, (C_p)_c, \theta_c)}{\partial c} \Delta c \cdot \sin \alpha_1 + \frac{\partial f(m_c, (k_3)_c, c_c, (C_p)_c, \theta_c)}{\partial k_3} \Delta k_3 \cdot \sin \alpha_2 + \frac{\partial f(m_c, (k_3)_c, c_c, (C_p)_c, \theta_c)}{\partial C_p} \Delta C_p \cdot \sin \alpha_3 + \frac{\partial f(m_c, (k_3)_c, c_c, (C_p)_c, \theta_c)}{\partial \theta} \Delta \theta \cdot \sin \alpha_3 \tag{34}$$

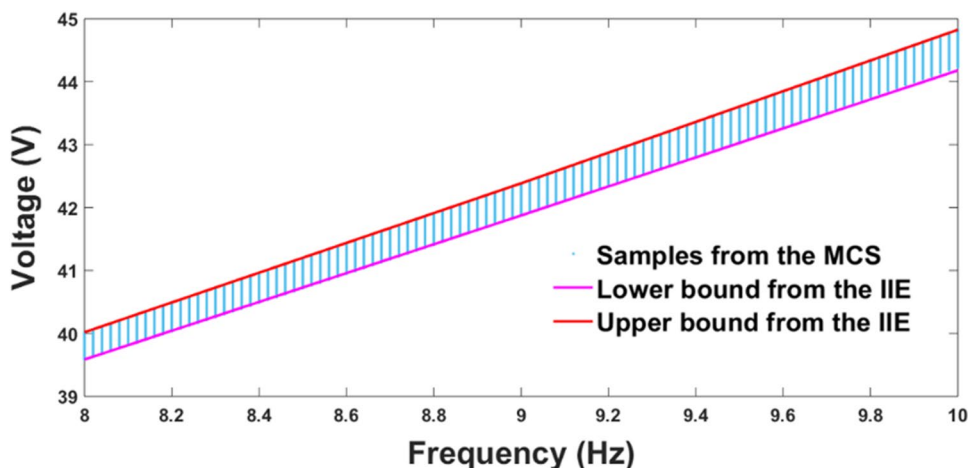
Therefore, the lower and upper bounds of the output voltage can be obtained:

$$f(m^l, k_3^l, c^l, C_p^l, \theta^l) = f(m_c, (k_3)_c, c_c, (C_p)_c, \theta_c) + \text{minimum}(G(\alpha_1, \alpha_2, \alpha_3)), \tag{35}$$

Table 2 The simulation cases

Case	Uncertain parameter	Level of excitation (m/s ²)
1	m^l	4
2	m^l, k_3^l, c^l	4
3	C_p^l, θ^l	4
4	$m^l, k_3^l, c^l, C_p^l, \theta^l$	4
5	$m^l, k_3^l, c^l, C_p^l, \theta^l$	5

Fig. 7 Bounds of the output voltage in case 1 (results obtained from improved interval extension—IIE and Monte Carlo simulations—MCS)



$$f(m^l, k_3^l, c^l, C_p^l, \theta^l) = f(m_c, (k_3)_c, c_c, (C_p)_c, \theta_c) + \text{maximum}(G(\alpha_1, \alpha_2, \alpha_3)). \quad (36)$$

The finite-difference method is used to calculate the sensitivities in above equations. The bounds of the output voltage are obtained at the different cases, and these cases are described in Table 2.

Firstly, only the uncertain parameter m is considered, and it is expressed by the interval number m^l . The bounds of the output voltages are predicted by the IIE based on the first-order Taylor series, when the excitation frequency is 8 Hz, 9 Hz and 10.5 Hz (the excitation level is 4 m/s²). The lower and upper bounds of the output voltages under different excitation frequencies can be connected with line segments separately. The numerical results from case-1 are plotted in Fig. 7. In order to demonstrate the accuracy of the interval analysis, we assume the uncertain variables listed in Table 1 to be distributed uniformly within their intervals. Then, the Monte Carlo simulation (MCS) is carried out, and

the number of simulations is 10,000. In each simulation, the space of the excitation frequencies is 0.02 Hz. The samples obtained via the MCS are also plotted in the same graph with bounds from the IIE. It is found that the samples are all distributed within the bounds from the IIE. This shows that the IIE can obtain the accurate bounds of the output voltage with the much less cost of calculation than the MCS.

In case 2, the uncertain structural parameters m , k_3 and c are taken into consideration. The interval analysis and the MCS are conducted, and the results are plotted in Fig. 8. It shows that the bounds of the output voltage from the IIE matches well with that from the MCS. The interval of the output voltage becomes wider as the number of uncertainties is increased from 1 to 3.

In case 3, the uncertain electric parameters C_p and θ are considered, as the results shown in Fig. 9. Comparing with the results in Fig. 8, it is found that the interval in Fig. 9 is wider than that in Fig. 8. This means that the uncertain electric parameters have a stronger influence on the output voltage of the BEH than the uncertain structural parameters.

Fig. 8 Bounds of the output voltage in case 2

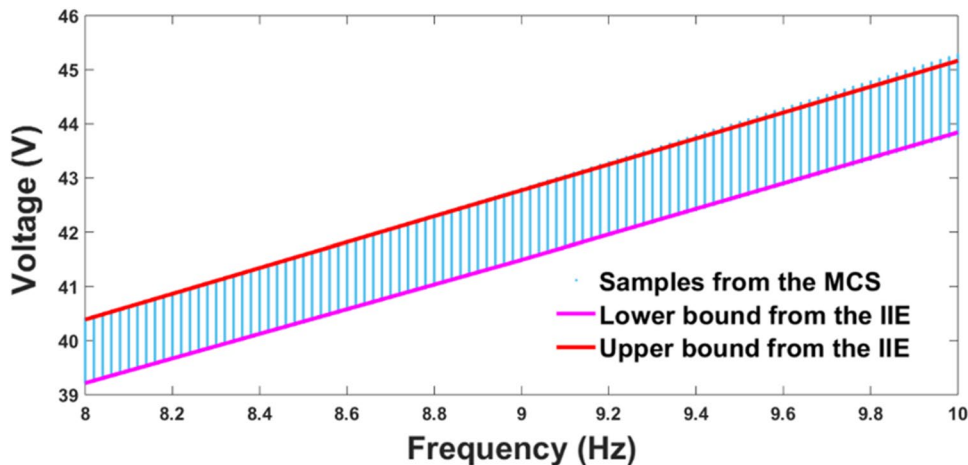


Fig. 9 Bounds of the output voltage in case 3

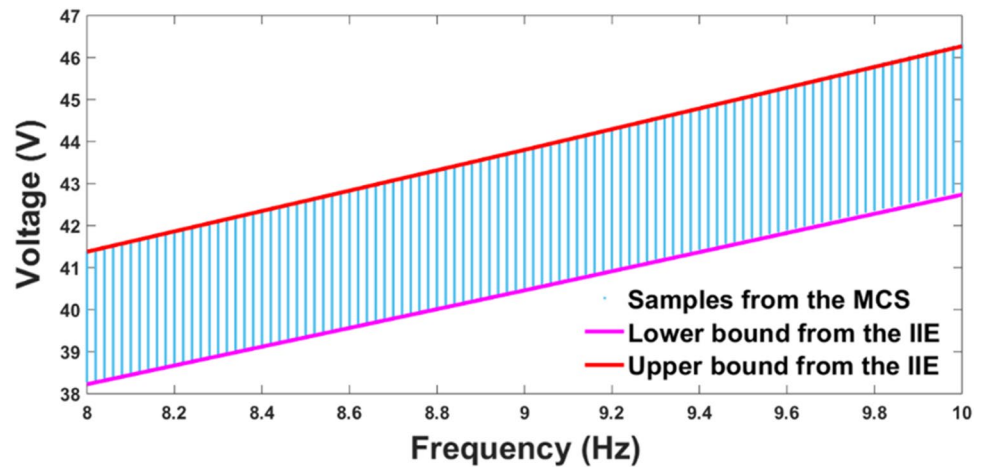


Fig. 10 Bounds of the output voltage in case 4

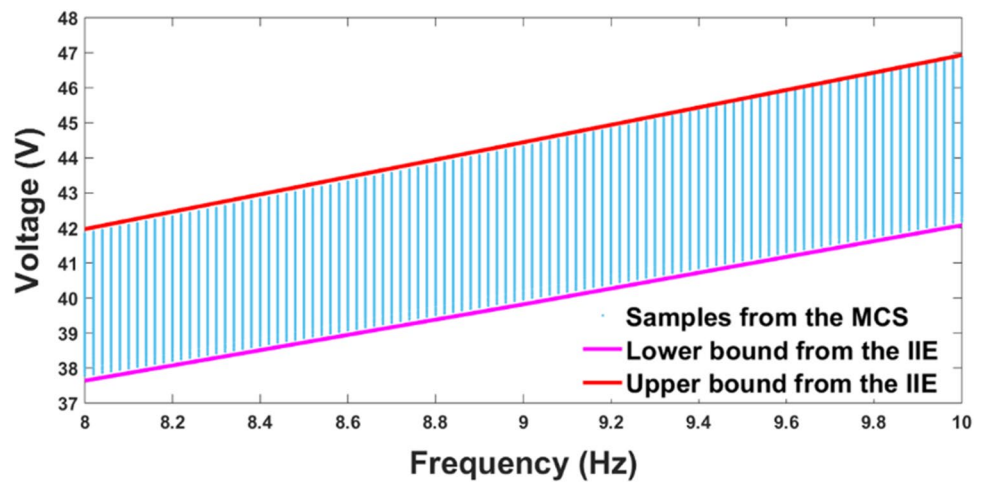
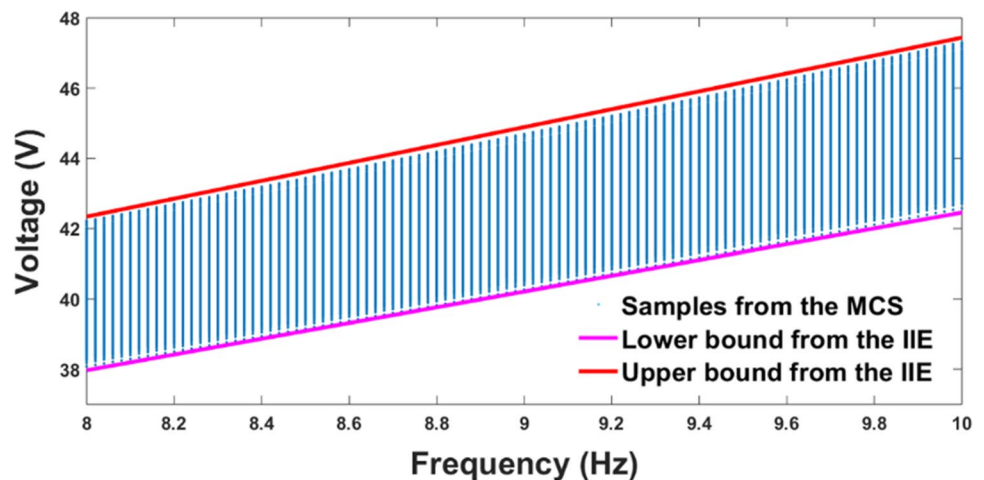


Fig. 11 Bounds of the output voltage in case 5



Finally, we take all five uncertain parameters listed in Table 1 into consideration and carry out simulations at different excitation levels (4 m/s^2 in case 4; 5 m/s^2 in case 5). Note that the acceleration levels 4 m/s^2 and 5 m/s^2 are large enough to ensure the large amplitude oscillation of the BEH.

The results show that the accuracy of the interval analysis is good, and the width of the interval is almost same for different excitation levels. However, the central value slightly moves up at the high level of excitation (5 m/s^2), as shown in Figs. 10 and 11. From the uncertain analysis [20, 21],

it is found that the higher vibration orbit of the nonlinear energy harvesters needs the higher excitation level. From above uncertain analysis, which parameter leads to a higher vibration orbit can be determined. Therefore, the nonlinear energy harvesters can be designed based on the real-application environments.

Conclusions

This paper uses the improved interval extension based on the first-order Taylor series to predict the lower and upper bounds of the stable high-energy interwell output voltage of the BEH with uncertain mass, nonlinear stiffness term, damping, capacitance and electromechanical coupling coefficient. Meanwhile, the Monte Carlo simulation is used to verify the suitability and the accuracy of this method. Particularly, this method allows researchers to define the number of parameter α_i according to the categories of uncertain variables. For example, the structural uncertainties and the electrical uncertainties should be expressed by two parameters α_1 and α_3 . Consequently, accurate bounds of output voltage can be predicted. It is found that interval of the output voltage of the BEH can be limited by reducing the number of uncertain variables, and the bounds of the output voltage is more sensitive to the electrical uncertain variables than the structural uncertainties. Therefore, designers of the BEH should pay enough attention on the errors and tolerances of the electrical output design variables. Specifically, in the design of the BEH, it is more effective to improve the accuracy of the output voltage by limiting the uncertainties of electric parameters than structural parameters. Reducing the number of uncertain parameters through increasing processing precision in production of the BEH can also improve the accuracy of the output voltage.

Acknowledgements This work was supported by the National Natural Science Foundation of China (Grant no. 11802237), the Fundamental Research Funds for the Central Universities (Grant no. G2018KY0306) and Foundation of Key Laboratory (Grant no. 61423010301).

Open Access This article is distributed under the terms of the Creative Commons Attribution 4.0 International License (<http://creativecommons.org/licenses/by/4.0/>), which permits unrestricted use, distribution, and reproduction in any medium, provided you give appropriate credit to the original author(s) and the source, provide a link to the Creative Commons license, and indicate if changes were made.

References

- Nandi S, Toliyat HA, Li X (2010) Condition monitoring and fault diagnosis of electrical motors—a review. *IEEE Trans Energy Convers* 20(4):719–729
- Li Y, Yang Y, Li G, Xu M, Huang W (2017) A fault diagnosis scheme for planetary gearboxes using modified multi-scale symbolic dynamic entropy and mRMR feature selection. *Mech Syst Signal Proc* 91:295–312
- Li Y, Li G, Yang Y, Liang X, Xu M (2018) A fault diagnosis scheme for planetary gearboxes using adaptive multi-scale morphology filter and modified hierarchical permutation entropy. *Mech Syst Signal Proc* 105:319–337
- Li Y, Wang X, Si S, Huang S (2019) Entropy based fault classification using the Case Western Reserve University data: a benchmark study. *IEEE Trans Reliab*. <https://doi.org/10.1109/TR.2019.2896240>
- Ottman GK, Hofmann HF, Bhatt AC, Lesieutre GA (2002) Adaptive piezoelectric energy harvesting circuit for wireless remote power supply. *IEEE Trans Power Electr* 17(5):669–676
- Yang Z, Zhou S, Zu J, Inman DJ (2018) High-Performance piezoelectric energy harvesters and their applications. *Joule* 2(4):642–697
- Li Y, Feng K, Liang X, Zuo MJ (2018) A fault diagnosis method for planetary gearboxes under non-stationary working conditions using improved Vold–Kalman filter and multi-scale sample entropy. *J Sound Vib* 439:271–286
- Giurgiutiu V, Zagari A, Bao J (2002) Piezoelectric wafer embedded active sensors for aging aircraft structural health monitoring. *Struct Health Monit* 1(1):41–61
- Akaydin HD, Elvin N, Andreopoulos Y (2010) Energy harvesting from highly unsteady fluid flows using piezoelectric materials. *J Intell Mater Syst Struct* 21(13):1263–1278
- Kwuimy CAK, Litak G, Borowiec M, Nataraj C (2012) Performance of a piezoelectric energy harvester driven by air flow. *Appl Phys Lett* 100(2):024103
- Zhao L, Tang L, Yang Y (2013) Comparison of modeling methods and parametric study for a piezoelectric wind energy harvester. *Smart Mater Struct* 22(12):125003
- Zhou S, Wang J (2018) Dual serial vortex-induced energy harvesting system for enhanced energy harvesting. *AIP Adv* 8:075221
- Dai H, Abdelmoula H, Abdelkefi A, Wang L (2017) Towards control of cross-flow-induced vibrations based on energy harvesting. *Nonlinear Dyn* 88(4):2329–2346
- Song R, Shan X, Lv F, Xie T (2015) A study of vortex-induced energy harvesting from water using PZT piezoelectric cantilever with cylindrical extension. *Ceram Int* 41:768–773
- Wang J, Zhou S, Zhang Z, Yurchenko D (2019) High-performance piezoelectric wind energy harvester with Y-shaped attachments. *Energy Convers Manag* 181:645–652
- Chen L, Jiang W (2015) Internal resonance energy harvesting. *J Appl Mech Trans ASME* 82(3):031004
- Chen L, Jiang W, Panyam M, Daqaq MF (2016) A broadband internally resonant vibratory energy harvester. *J Vib Acoust* 138(6):061007
- Harne RL, Wang KW (2013) A review of the recent research on vibration energy harvesting via bistable systems. *Smart Mater Struct* 22(2):023001
- Lee AJ, Inman DJ (2018) A multifunctional bistable laminate: snap-through morphing enabled by broadband energy harvesting. *J Intell Mater Syst Struct* 29(11):2528–2543
- Zhou S, Cao J, Inman DJ, Lin J, Liu S, Wang Z (2014) Broadband tristable energy harvester: modeling and experiment verification. *Appl Energy* 133:33–39
- Zhou S, Zuo L (2018) Nonlinear dynamic analysis of asymmetric tristable energy harvesters for enhanced energy harvesting. *Commun Nonlinear Sci* 61:271–284
- Zhou Z, Qin W, Zhu P (2017) A broadband quad-stable energy harvester and its advantages over bi-stable harvester: simulation and experiment verification. *Mech Syst Signal Proc* 84:158–168

23. Huang D, Zhou S, Litak G (2019) Nonlinear analysis of multi-stable energy harvesters for enhanced energy harvesting. *Commun Nonlinear Sci* 69:270–286
24. Erturk A, Inman DJ (2011) Broadband piezoelectric power generation on high-energy orbits of the bistable Duffing oscillator with electromechanical coupling. *J Sound Vib* 330(10):2339–2353
25. Zhou S, Cao J, Erturk A, Lin J (2013) Enhanced broadband piezoelectric energy harvesting using rotatable magnets. *Appl Phys Lett* 102(17):173901
26. Cao J, Wang W, Zhou S, Inman DJ, Lin J (2015) Nonlinear time-varying potential bistable energy harvesting from human motion. *Appl Phys Lett* 107(14):143904
27. Litak G, Friswell MI, Adhikari S (2010) Magnetopiezoelectric energy harvesting driven by random excitations. *Appl Phys Lett* 96(21):214103
28. Stanton SC, McGehee CC, Mann BP (2010) Nonlinear dynamics for broadband energy harvesting: investigation of a bistable piezoelectric inertial generator. *Phys D* 239(10):640–653
29. Arrieta AF, Hagedorn P, Erturk A, Inman DJ (2010) A piezoelectric bistable plate for nonlinear broadband energy harvesting. *Appl Phys Lett* 97(10):104102
30. Ali SF, Friswell MI, Adhikari S (2010) Piezoelectric energy harvesting with parametric uncertainty. *Smart Mater Struct* 19:105010
31. Franco VR, Varoto PS (2017) Parameter uncertainties in the design and optimization of cantilever piezoelectric energy harvesters. *Mech Syst Signal Proc* 93:593–609
32. Mann BP, Barton DA, Owens BA (2012) Uncertainty in performance for linear and nonlinear energy harvesting strategies. *J Intell Mater Syst Struct* 23:1451–1460
33. Pownuk A (2004) Efficient method of solution of large scale engineering problems with interval parameters based on sensitivity analysis. In: *Proceeding of NSF workshop on reliable engineering computing*, September 15–17, Savannah, Georgia, USA, pp 305–316
34. Chen SH, Wu J, Chen YD (2004) Interval optimization for uncertain structures. *Finite Elem Anal Des* 40:1379–1398
35. Li Y, Xu YL (2018) Increasing accuracy in the interval analysis by the improved format of interval extension based on the first order Taylor series. *Mech Syst Signal Process* 104:744–757
36. Li Y, Wang TH (2018) Interval analysis of the wing divergence. *Aerosp Sci Technol* 74:17–21
37. Li Y, Zhou S, Litak G (2019) Uncertainty analysis of excitation conditions on performance of nonlinear monostable energy harvesters. *Int J Struct Stab Dyn* 19(6):1950052
38. Erturk A, Inman DJ (2011) *Piezoelectric energy harvesting*. Wiley, New York
39. Zhou S, Cao J, Lin J (2016) Theoretical analysis and experimental verification for improving energy harvesting performance of nonlinear monostable energy harvesters. *Nonlinear Dyn* 86(3):1599–1611
40. Elishakoff I, Miglis Y (2012) Novel parameterized intervals may lead to sharp bounds. *Mech Res Commun* 44:1–8
41. Elishakoff I, Thakkar K (2014) Overcoming overestimation characteristic to classical interval analysis. *AIAA J* 52:2093–2097

Publisher's Note Springer Nature remains neutral with regard to jurisdictional claims in published maps and institutional affiliations.